

# **Neutron star masses, radii, and the dense-matter equation of state**

## **Lecture 2**

**Carolyn Raithel**

**Institute for Advanced Study**

**Princeton University**

**July 24, 2023**

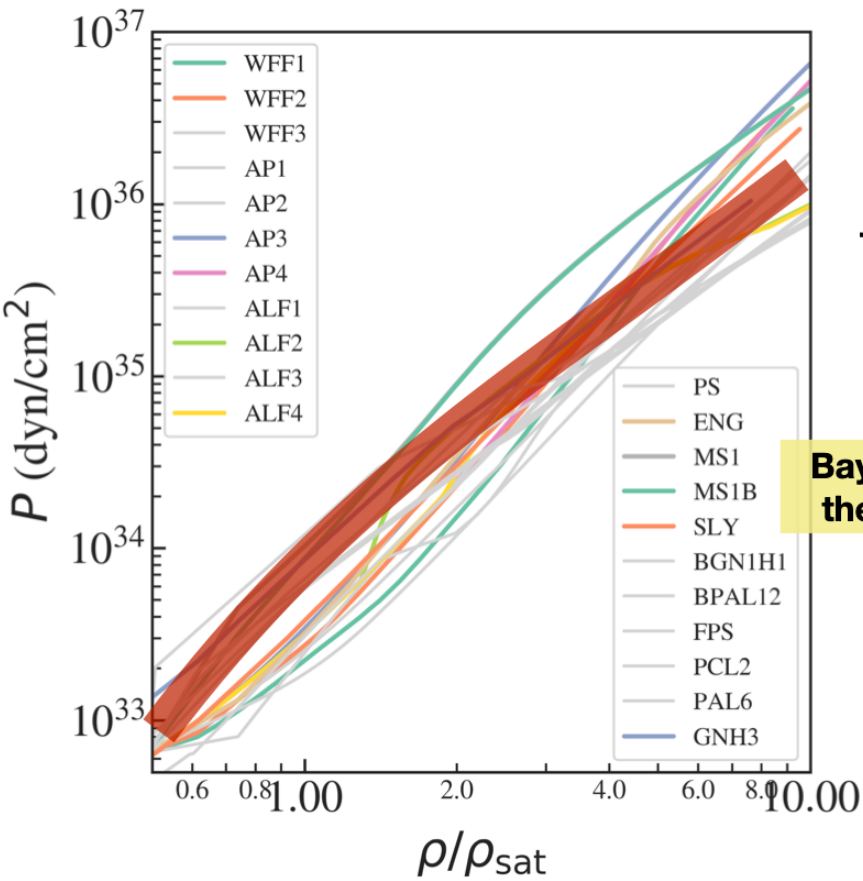


**19th International Conference on  
QCD in Extreme Conditions (XQCD 2023)**

**FLAD**

LUSO-AMERICAN  
DEVELOPMENT  
FOUNDATION

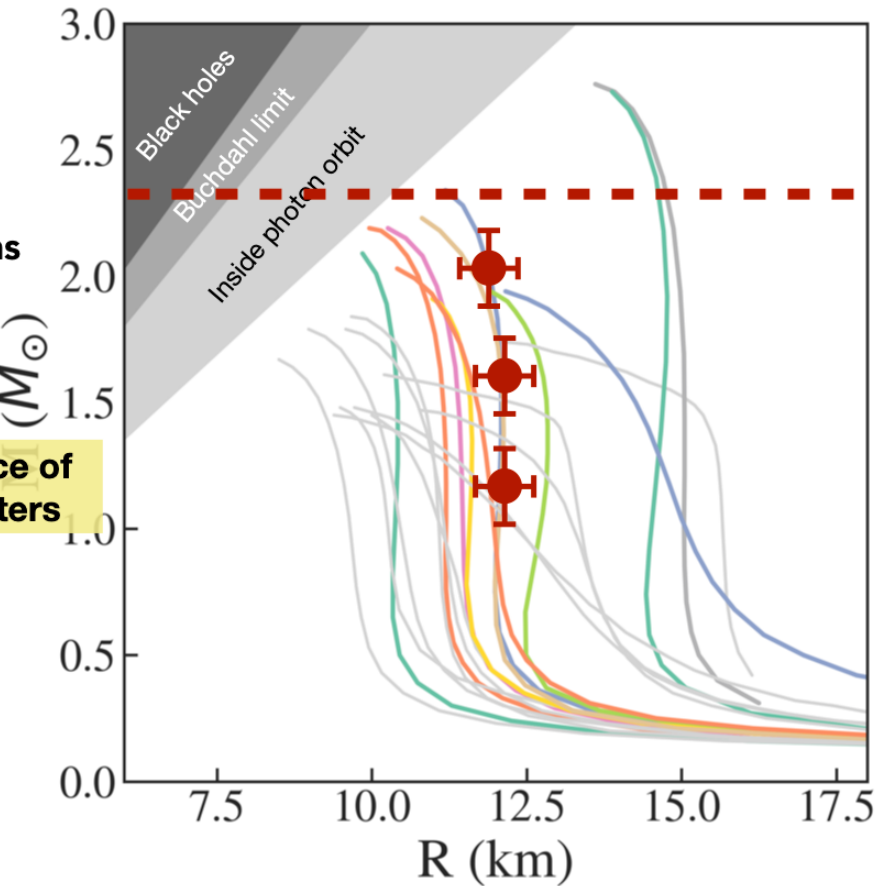
# Mass-radius relations for theoretical EOSs



TOV equations



Bayesian inference of  
the EOS parameters

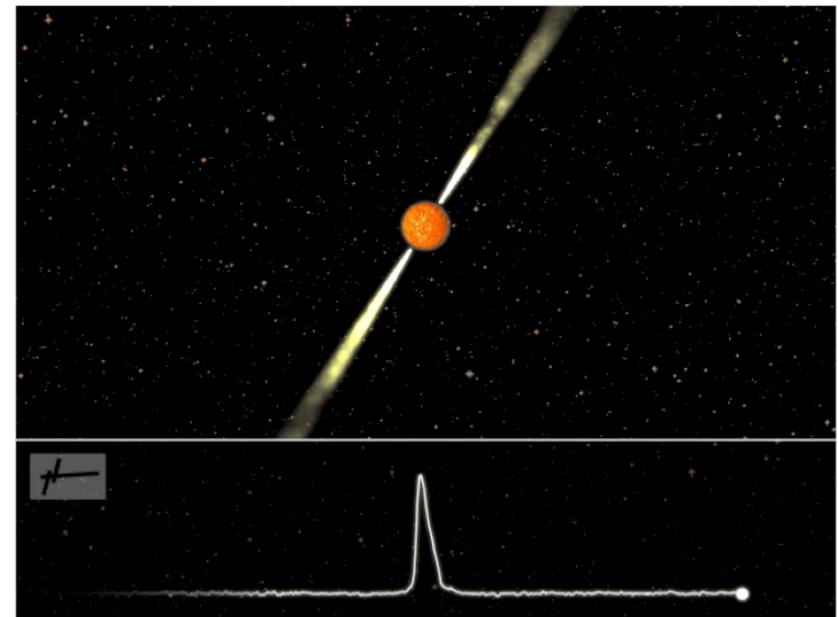
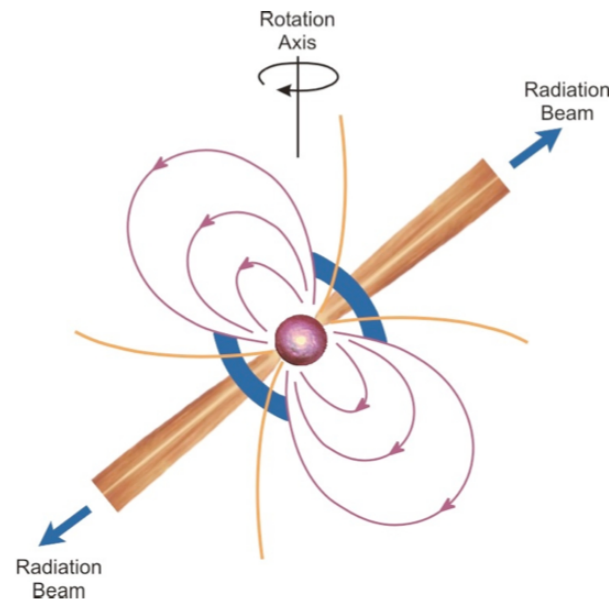


# Rotation-powered pulsars

Rapidly rotating neutron stars that emit beamed emission along their magnetic axis

First pulsar discovered in 1967 by Jocelyn Bell and Anthony Hewish

**>3,300 now known**



Video credit: Joeri Van Leeuwen

# Pulsar “ $P$ – $\dot{P}$ ” Diagram

Assuming all of the spin-down is due to magnetic dipole braking:

$$B \propto \sqrt{P\dot{P}}$$

$$\tau \propto \frac{P}{\dot{P}}$$

For  $\dot{P} = 10^{-20} \text{ s/s}$ ,  
changing the period by  
**1 ns** would take  $10^{11} \text{ s}$   
or **3,171 years!**

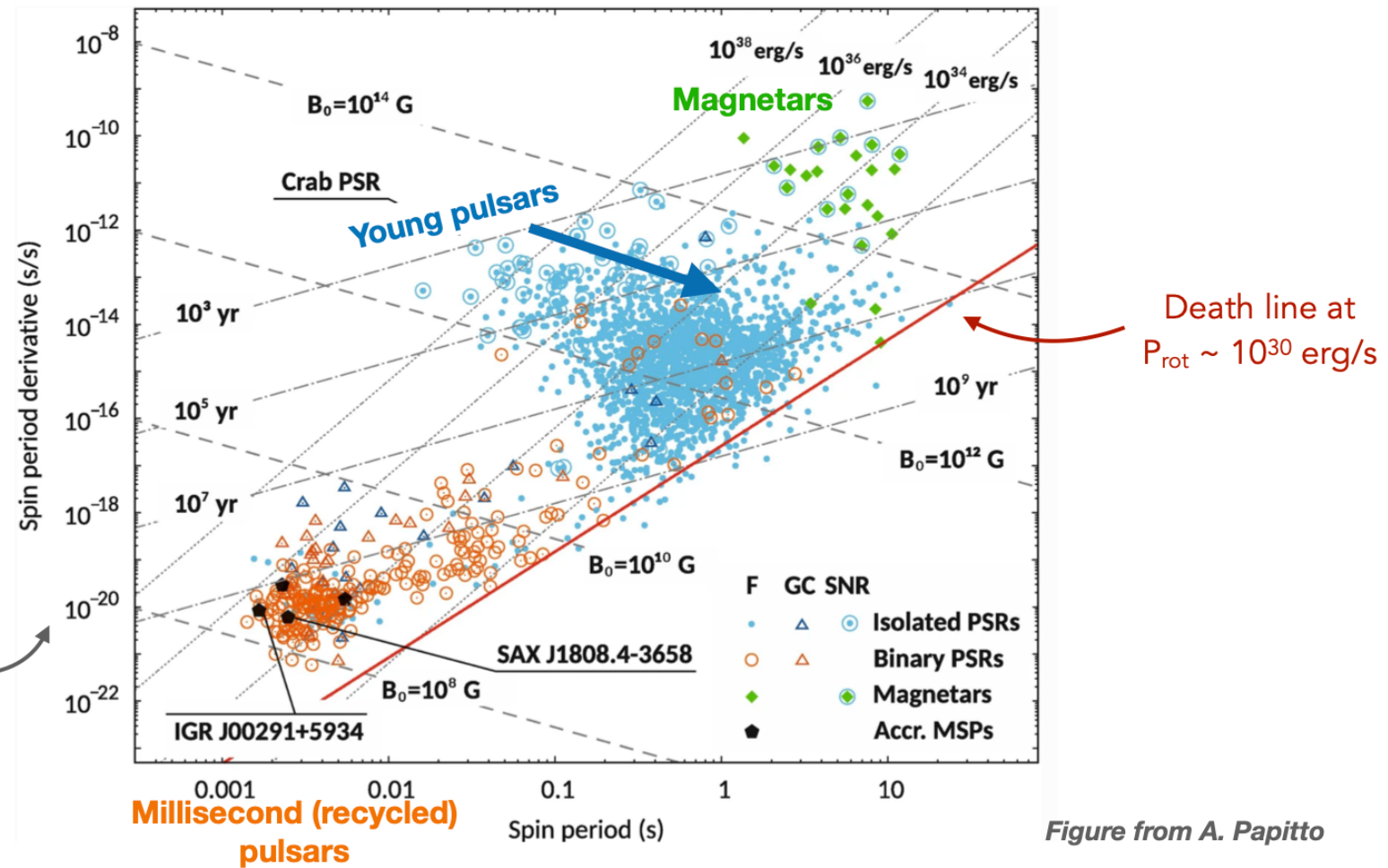


Figure from A. Papitto

# Post-Keplerian parameters

Potentially observable relativistic effects in pulsar timing:

## 1. Advance of the periastron

analogous to perihelion advance of Mercury

● Requires high eccentricity

## 2. Einstein delay

due to gravitational redshift and time dilatation

● Requires high eccentricity

## 3. Shapiro delay

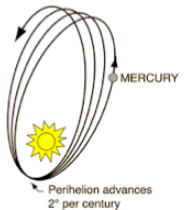
due to propagation of signal through curved spacetime of companion

● Requires nearly edge-on orbits

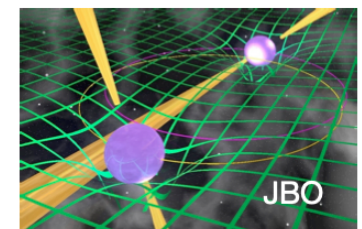
## 4. Orbital decay

via gravitational wave emission

$$\dot{\omega} \sim 40 \text{ deg yr}^{-1} \left( \frac{P_b}{\text{hr}} \right)^{-5/3} \left( \frac{1}{1 - e^2} \right) \left( \frac{m_p + m_c}{M_\odot} \right)^{2/3}$$



$$\gamma \sim 2.4 \text{ ms} \left( \frac{P_b}{\text{hr}} \right)^{1/3} e \frac{m_c(m_p + 2m_c)}{(m_p + m_c)^{4/3}}$$



$$r \sim 5 \mu\text{s} \times m_c$$

$$s = \sin i \sim 0.9 \left( \frac{P_b}{\text{hr}} \right)^{-2/3} x \frac{(m_p + m_c)^{2/3}}{m_c}$$

$$\dot{P}_b \sim -4 \times 10^{-12} \left( \frac{P_b}{\text{hr}} \right)^{-5/3} \frac{\left( 1 + \frac{73}{24}e^2 + \frac{37}{96}e^4 \right)}{(1 - e^2)^{7/2}} \frac{m_p m_c}{(m_p + m_c)^{1/3}}$$

● Requires many years of timing and very compact orbits ( $P_b \lesssim 1$  day)

# Double Pulsar System: J0737-3039A/B

Latest results from Kramer et al. (Phys Rev X, 2021)

## Timing parameters for PSR A

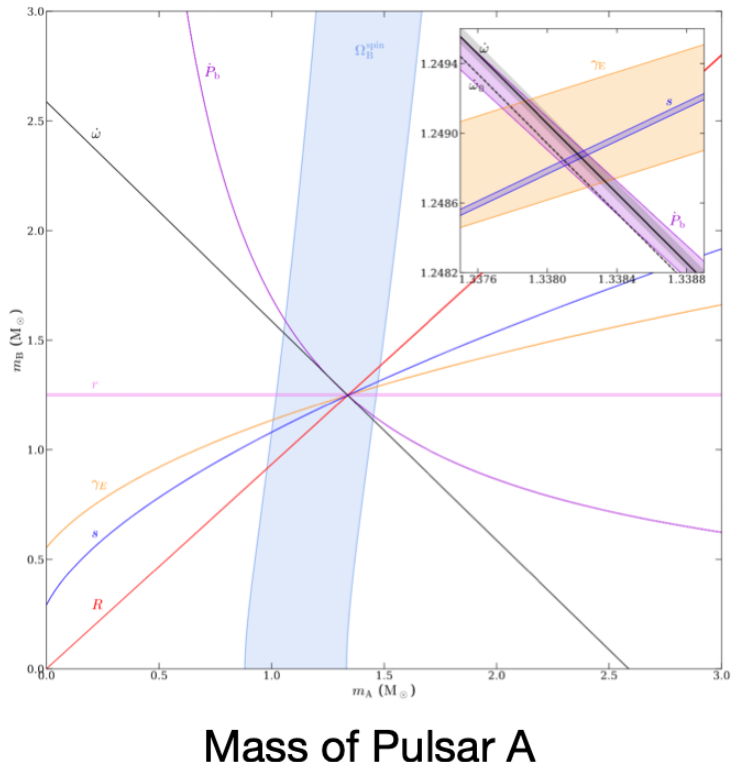
Parameter	Value
Right ascension, $\alpha$ (J2000)	07 <sup>h</sup> 37 <sup>m</sup> 51 <sup>s</sup> 248115(10) <sup>†</sup>
Declination, $\delta$ (J2000)	-30°39'40"70485(17) <sup>†</sup>
Proper motion R.A., $\mu_\alpha$ (mas yr <sup>-1</sup> )	-2.567(30) <sup>†</sup>
Proper motion Dec., $\mu_\delta$ (mas yr <sup>-1</sup> )	2.082(38) <sup>†</sup>
Parallax, $\pi_c$ (mas)	1.36(+0.12, -0.10) <sup>†</sup>
Position epoch (MJD)	55045.0000
Rotational frequency, $\nu$ (Hz)	44.05406864196281(17) <sup>‡</sup>
First freq. derivative, $\dot{\nu}$ (Hz s <sup>-1</sup> )	-3.4158071(11) $\times 10^{-15}$ <sup>‡</sup>
Second freq. derivative, $\ddot{\nu}$ (Hz s <sup>-2</sup> )	-2.286(29) $\times 10^{-27}$ <sup>‡</sup>
Third freq. derivative, $\dddot{\nu}$ (Hz s <sup>-3</sup> )	1.28(26) $\times 10^{-36}$ <sup>‡</sup>
Fourth freq. derivative, $\ddot{\ddot{\nu}}$ (Hz s <sup>-4</sup> )	4.580(86) $\times 10^{-43}$ <sup>‡</sup>
Timing epoch, $t_0$ (MJD)	55700.0
Profile evolution, FD parameter $c_1$	0.0000180(75)
Profile evolution, FD parameter $c_2$	-0.0001034(10)
Profile evolution, FD parameter $c_3$	0.0000474(26)
Dispersion measure, DM (pc cm <sup>-3</sup> )	48.917208
Orbital period, $P_o$ (day)	0.1022515592973(10) = 2h 27m
Projected semimajor axis, $x$ (s)	1.415028603(92)
Eccentricity (Kepler equation), $e_T$	0.087777023(61)
Epoch of periastron, $T_0$ (MJD)	55700.233017540(13)
Longitude of periastron, $\omega_0$ (deg)	204.753686(47)
Periastron advance, $\dot{\omega}$ (deg yr <sup>-1</sup> ) #	16.899323(13)
Change of orbital period, $\dot{P}_b$	-1.247920(78) $\times 10^{-12}$
Einstein delay amplitude, $\gamma_E$ (ms)	0.384045(94)
Logarithmic Shapiro shape, $z_s$	9.65(15)
Range of Shapiro delay, $r$ ( $\mu$ s)	6.162(21)
NLO factor for signal prop., $\eta_{\text{NLO}}$	1.15(13)
Relativistic deformation of orbit, $\delta_o$	13(13) $\times 10^{-6}$
Change of proj. semimajor axis, $\dot{x}$	8(7) $\times 10^{-16}$
Change of eccentricity, $\dot{e}_T$ (s <sup>-1</sup> )	3(6) $\times 10^{-16}$
Derived parameters	
$\sin i = 1 - \exp(-z_s)$	0.999936(+9/-10)
Orbital inclination, $i$ (deg)	89.35(5) or 90.65(5)
Total mass, $M$ ( $M_\odot$ )*	2.587052(+9/-7)
Mass of pulsar A, $m_A$ ( $M_\odot$ )*	1.338185(+12/-14)
Mass of pulsar B, $m_B$ ( $M_\odot$ )*	1.248868(+13/-11)
Galactic longitude, $l$ (deg)	245.2357
Galactic latitude, $b$ (deg)	-4.5049
Proper motion in $l$ , $\mu_l$ (mas yr <sup>-1</sup> )	-3.066(35)
Proper motion in $b$ , $\mu_b$ (mas yr <sup>-1</sup> )	-1.233(31)
Distance from $\pi_c$ , $d$ (pc)	735(60)
Transverse velocity, $v_T$ (km s <sup>-1</sup> )	11.5(10)

## Keplerian parameters

## Post-Keplerian parameters

## Inferred masses

## Mass-Mass Diagram



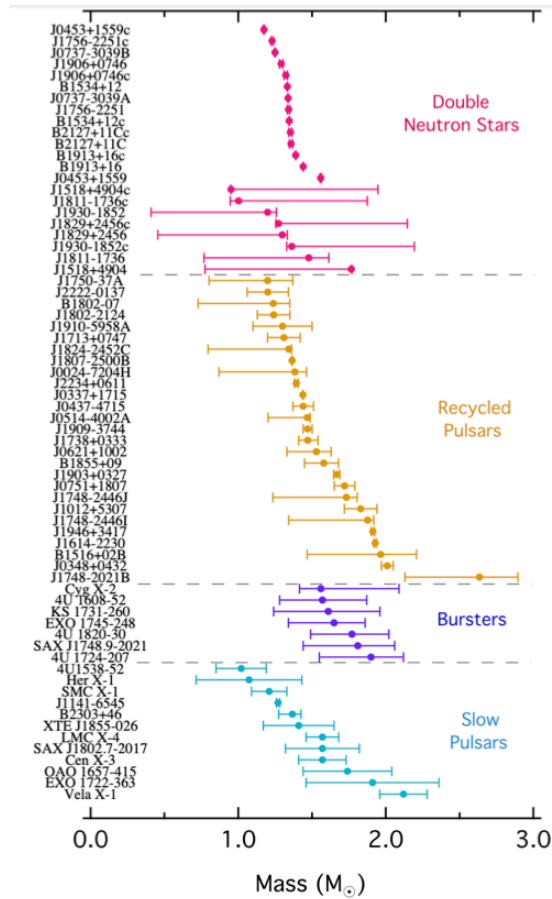
Mass of Pulsar B

Mass of Pulsar A

# Neutron star mass measurements

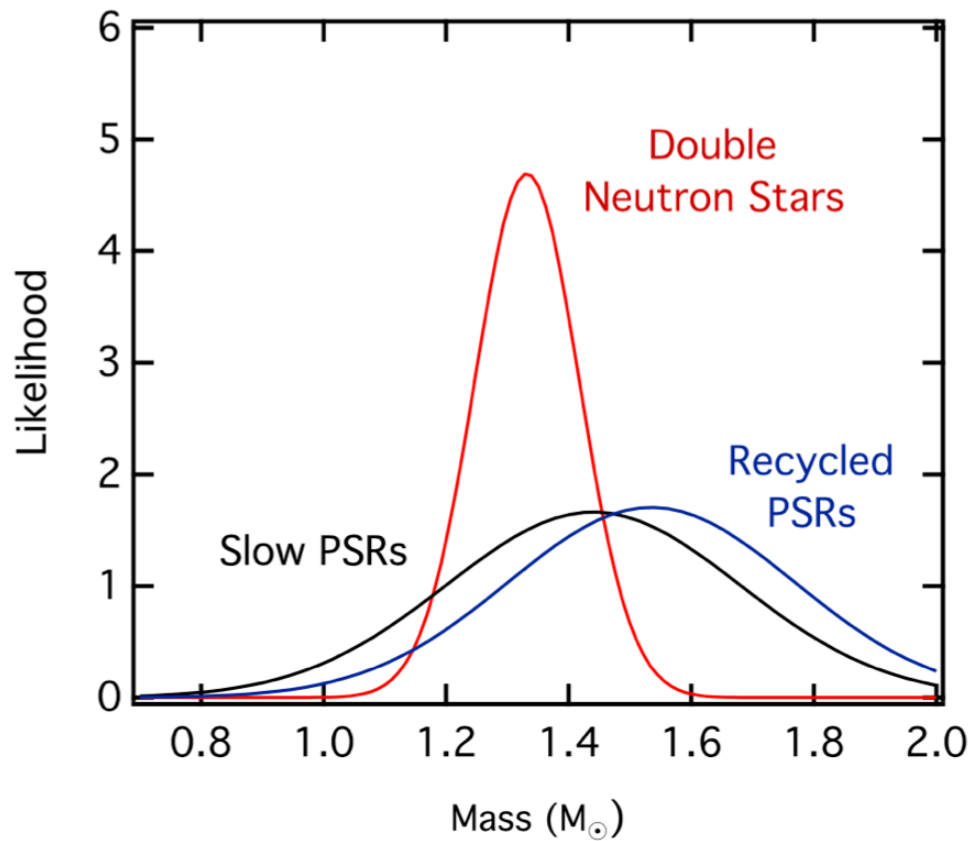
**Table 1 Masses of Double Neutron Star Systems and Non-recycled Pulsars**

System	$M_T$ ( $M_\odot$ )	$M_{\text{PSR}}$ ( $M_\odot$ )	$M_c$ ( $M_\odot$ )	Mass const.	Ref.
Systems with well-measured component masses					
J0453+1559	2.734(4)	1.559(5)	1.174(4)	$\dot{\omega}, h_3$	1,2
J0737-3039	2.58708(16)	1.3381(7)	1.2489(7) y	$\dot{\omega}, q$	3
B1534+12	2.678463(8)	1.3330(4)	1.3455(4)	$\dot{\omega}, \gamma$	4
J1756-2251	2.56999(6)	1.341(7)	1.230(7)	$\dot{\omega}, \gamma$	5
J1906+0746	2.6134(3)	1.291(11) y	1.322(11) ?	$\dot{\omega}, \gamma$	6
B1913+16	2.828378(7)	1.4398(2)	1.3886(2)	$\dot{\omega}, \gamma$	7
B2127+11C g	2.71279(13)	1.358(10)	1.354(10)	$\dot{\omega}, \gamma$	8
Systems with total binary mass measurement only					
J1518+4904	2.7183(7)	<1.768	>0.950	$\dot{\omega}$	9
J1811-1736	2.57(10)	<1.64	>0.93	$\dot{\omega}$	10
J1829+2456	2.59(2)	<1.34	>1.26	$\dot{\omega}$	11
J1930-1852	2.59(4)	<1.32	>1.30	$\dot{\omega}$	12
Non-recycled pulsars with massive WD companions					
J1141-6545	2.2892(3)	1.27(1) y	1.01(1)	$\dot{\omega}, \gamma$	14,15
B2303+46	2.64(5)	1.24-1.44 y	1.4-1.2	$\dot{\omega}, M_{\text{WD}}$	15,16



Review: Özel & Freire 2016

# Neutron star mass distribution



Özel & Freire 2016

# Massive pulsars

Previous record holders:

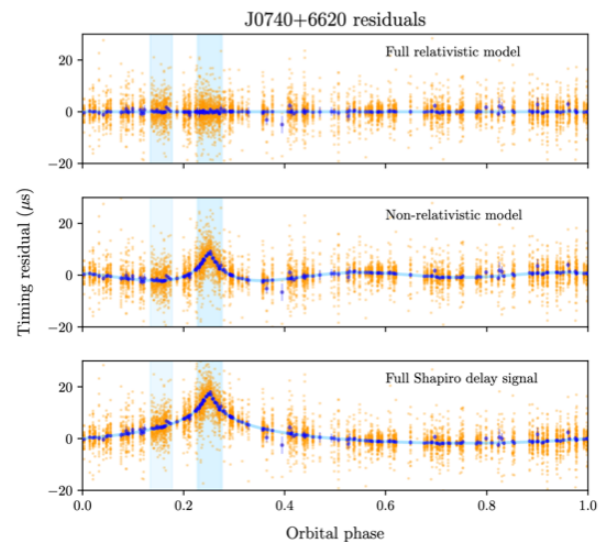
- J1614-2230:  $M = 1.928(7) M_{\odot}$  (Demorest et al. 2010)
- J0348+0432:  $M = 2.01(4) M_{\odot}$  (Antoniadis et al. 2013)

Current most massive pulsar: J0740+6620

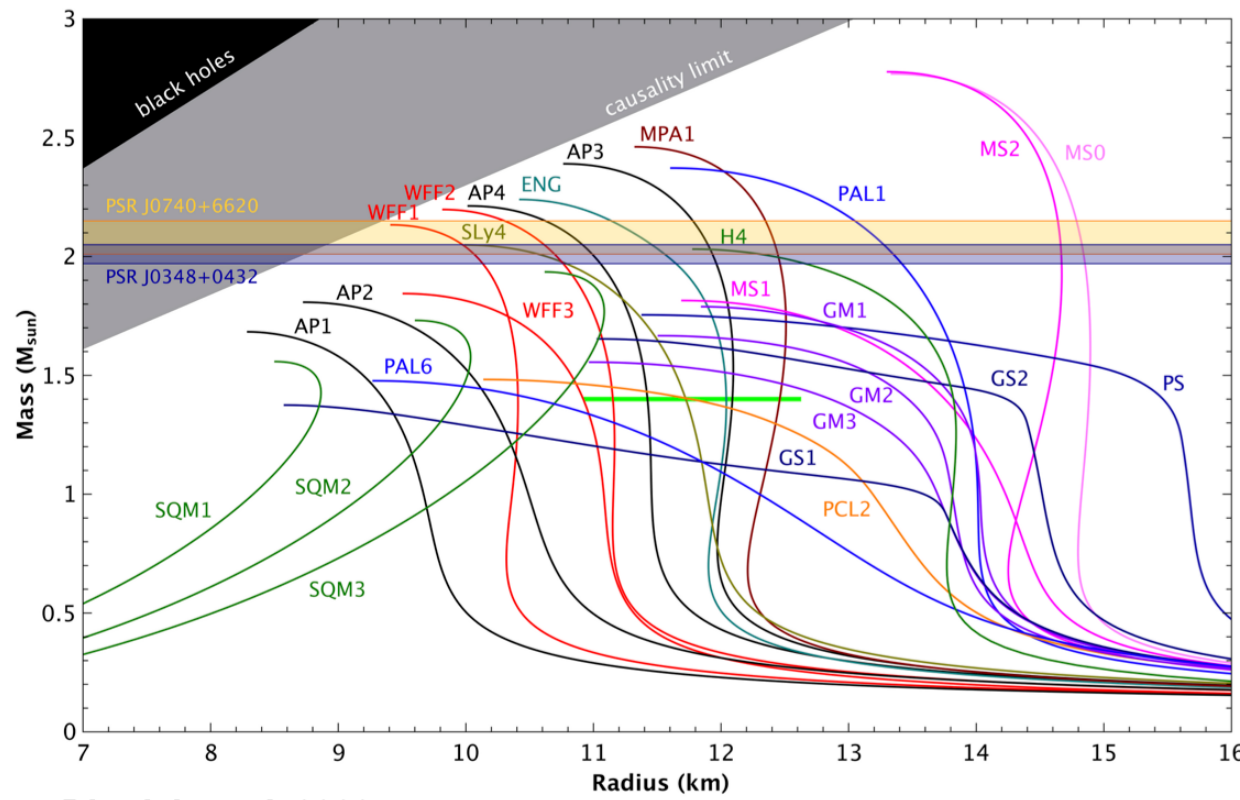
$$M = 2.08 \pm 0.07 M_{\odot}$$

(Cromartie et al. 2020; Fonseca et al. 2021)

Cromartie et al. 2020



# Massive pulsars and the equation of state



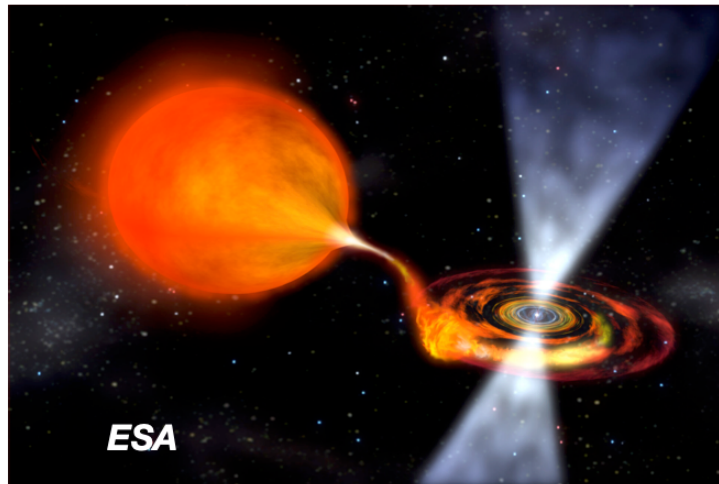
Existence of  $\sim 2 M_{\odot}$  neutron stars significantly **constrains soft EOSs**, e.g. those with new degrees of freedom appearing at high densities

↳ “hyperon puzzle” (e.g., Vidaña 2022 for a recent review)

# Measuring neutron star radii

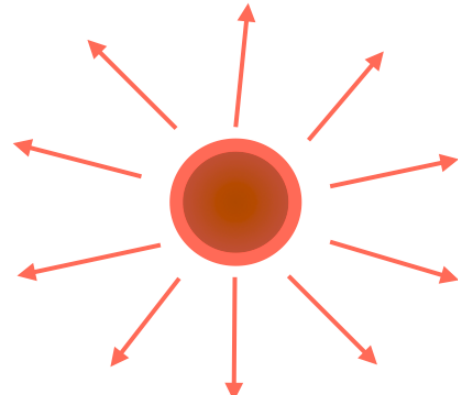
## ***Method I: Spectroscopy of NS surface emission***

Low-mass X-ray binary



*Accretion bombards surface and heats NS*

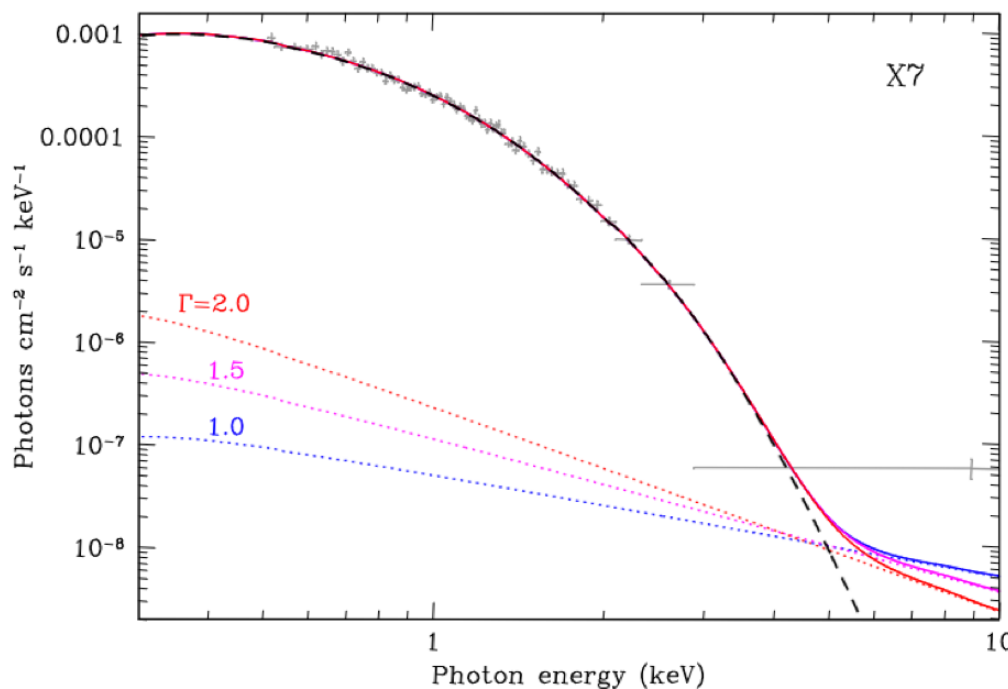
$$R^2 = \left( \frac{fD^2}{\sigma T^4} \right) \left( 1 - \frac{2GM}{Rc^2} \right)$$



*During quiescence, NS re-radiates stored heat*

# Spectroscopic neutron star radii during quiescence

Chandra X-ray spectrum for  
quiescent low-mass X-ray binary X7



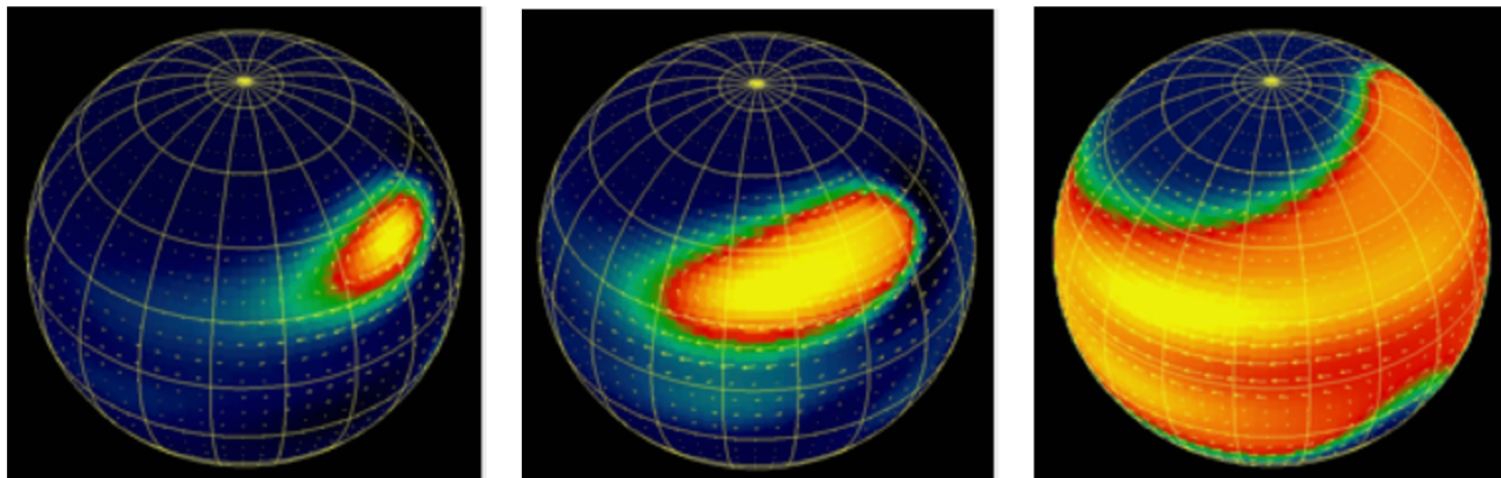
Fit atmosphere model to  
spectrum to measure  
*effective temperature*

Dotted lines = models for  
non-thermal contribution

Bogdanov et al. 2016

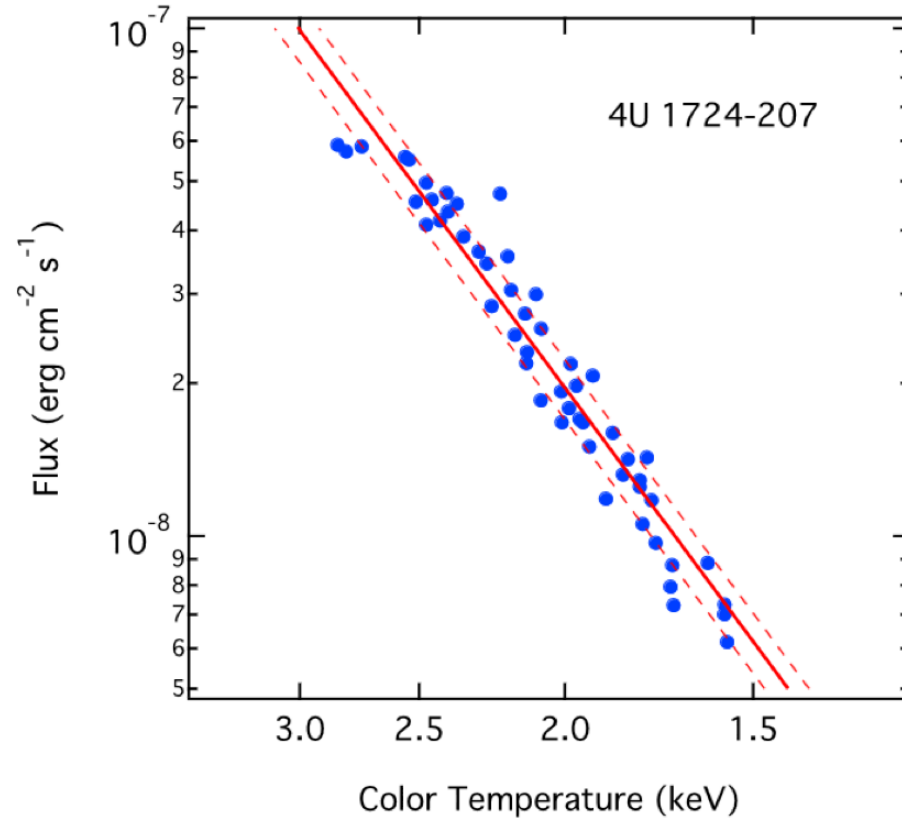
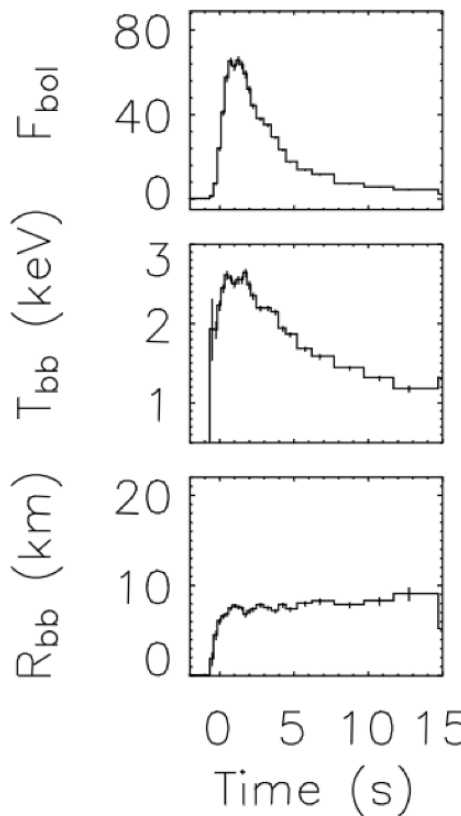
# Thermonuclear bursts

- Accreted material builds up and is compacted by surface gravity
- For high enough temperature, triple-a process ignites and burning rapidly spreads over surface of star ( $t \sim 1s$ )



*Simulation of flame spreading on NS surface  
from A. Spitkovsky*

# Thermonuclear burst data



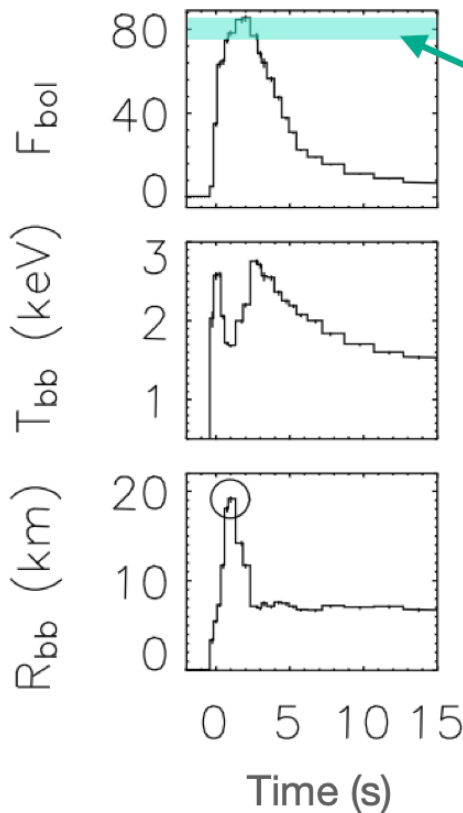
Left: An ordinary burst from 4U 1636+536 (Galloway et al. 2006); Right: Ozel et al. 2016

Flux  $\sim T^4$

Normalization  
gives the effective  
emitting area

Scatter from  
repeated events  
gives measure of  
uncertainty

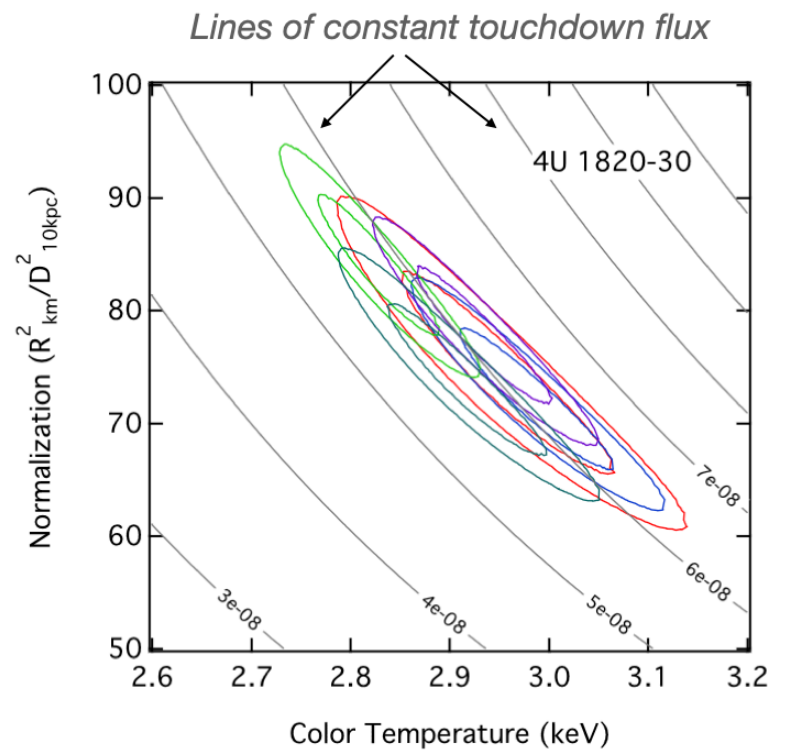
# Photospheric radius expansion (PRE) burst



**Eddington limit:**  
When radiative and  
gravitational forces balance

$$F_{\text{Edd}} = \frac{GMC}{k_{\text{es}} D^2} \left(1 - \frac{2GM}{Rc^2}\right)^{1/2}$$

Scattering opacity  $k_{\text{es}}$   
additionally depends  
on NS surface gravity

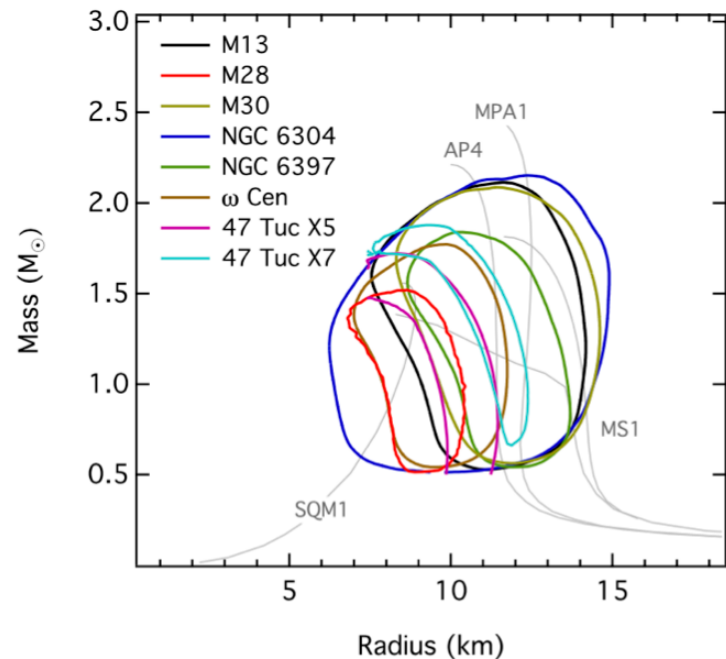


*Repeated bursts give consistent radii*

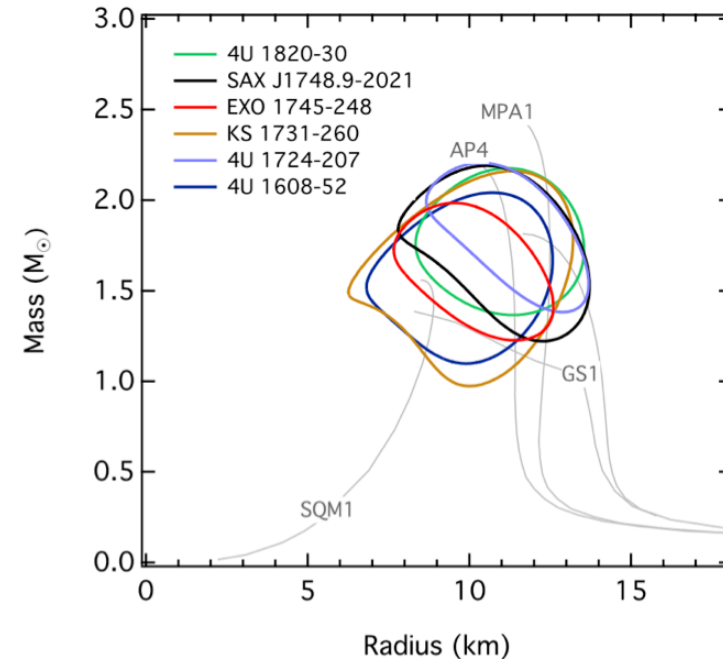
Left: An PRE burst from 4U 1636+536 (Galloway et al. 2006); Right: Ozel et al. 2016

# Spectroscopic radius constraints

8 sources during quiescence



6 burst sources

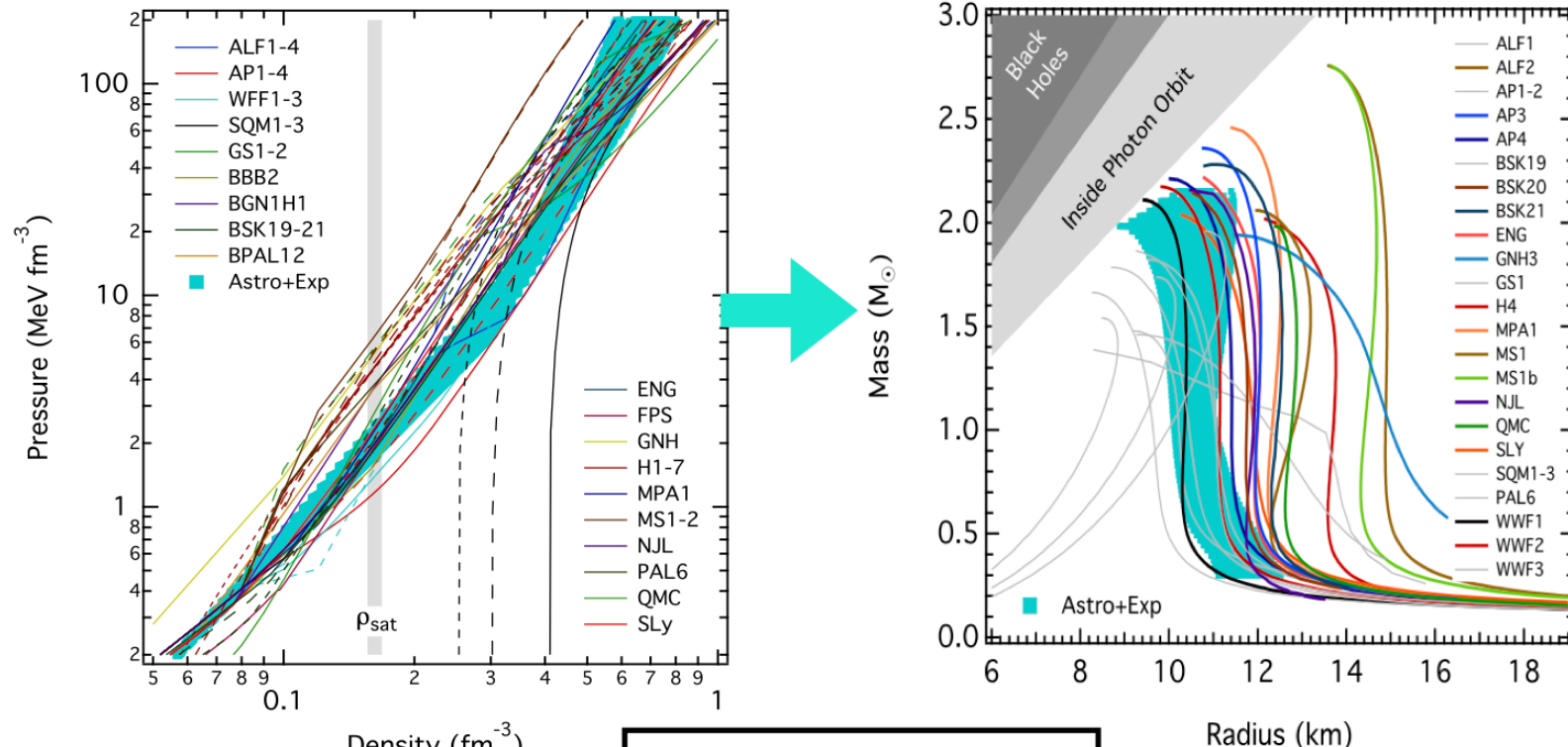


Özel et al. 2016

For a review, see Özel and Friere 2016

# Spectroscopic neutron star radii

Radius measurements combined via **Bayesian inference scheme**,  
*including data from low energy nuclear constraints + massive pulsars*

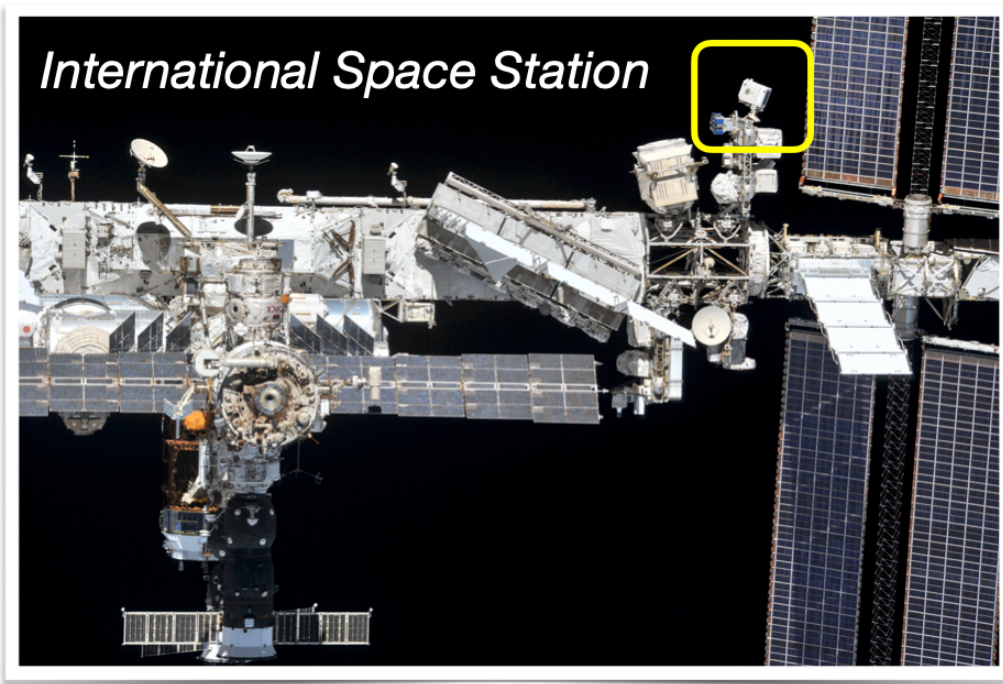


# Not a settled problem

How significant is the impact of residual accretion on inferred radii?

- e.g. Poutanen et al. 2014, Kajava et al. 2014 make different assumptions and generally find larger radii for the burst sources (~13 km)

# Method #2: Pulse profile modeling with NICER



# Pulse profile modeling

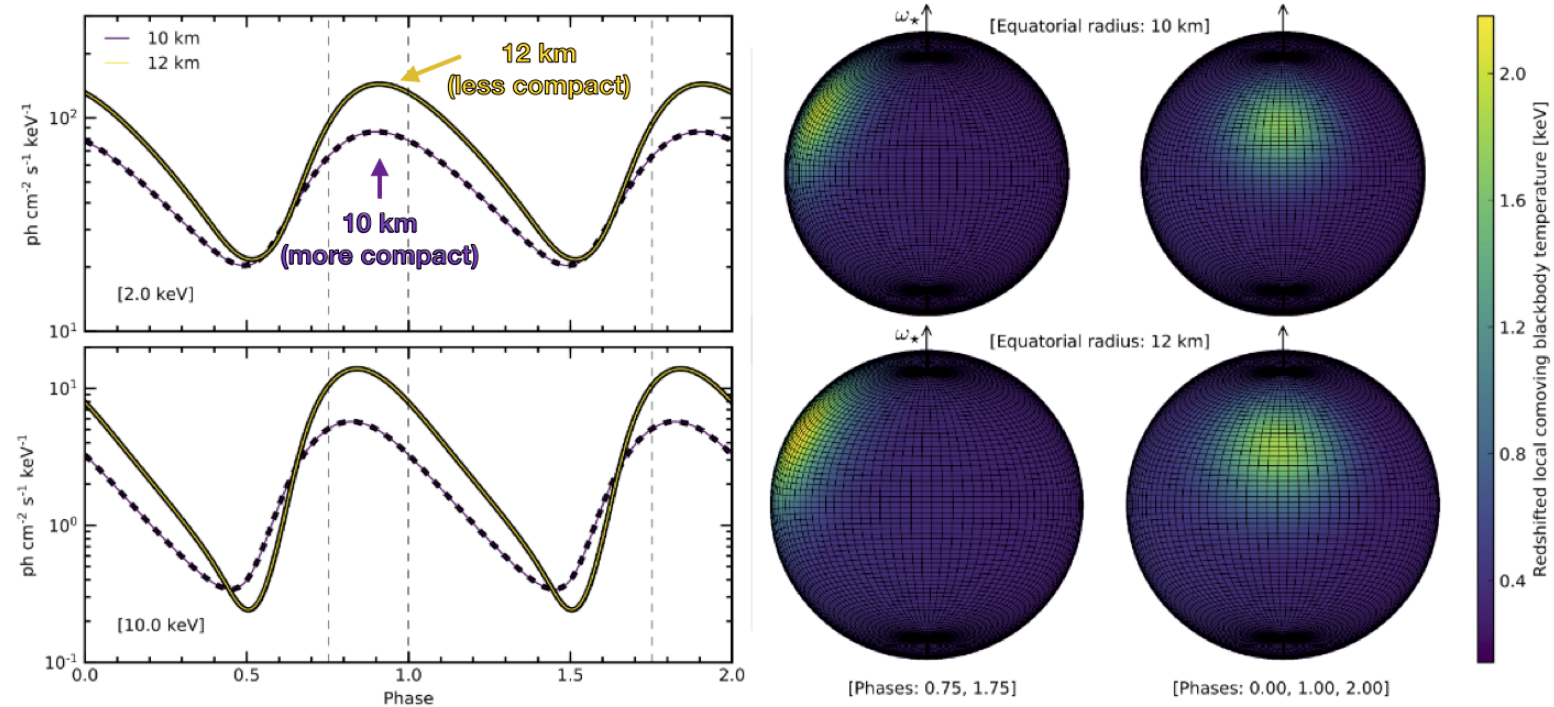
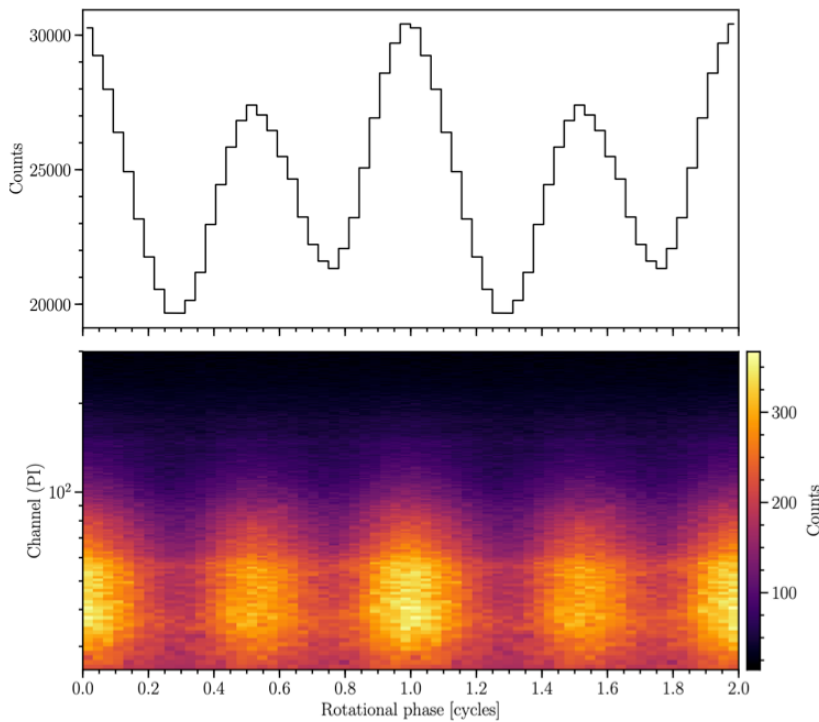


Figure from Watts 2017 (courtesy of Tom Riley)

# PSR J0030+0451

An isolated millisecond pulsar ( $f = 205$  Hz)

Riley et al. 2019

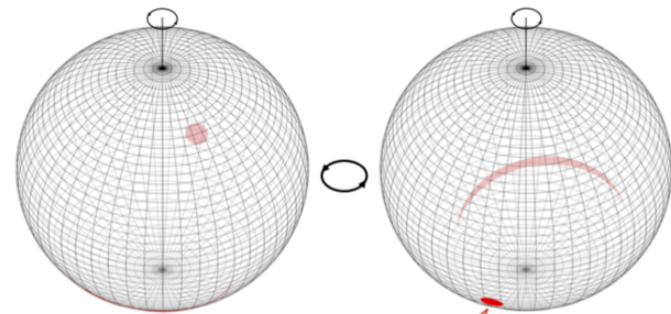


Best fit hotspot model from  
Riley et al. 2019

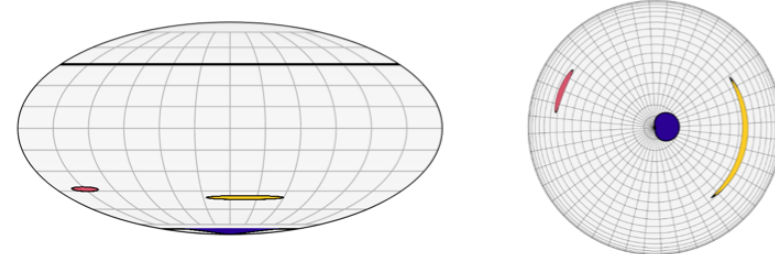
Northern rotational hemisphere  
(viewed at Earth inclination)

$$\phi \in \mathbb{Z}$$

$$\left(\phi - \frac{1}{2}\right) \in \mathbb{Z}$$



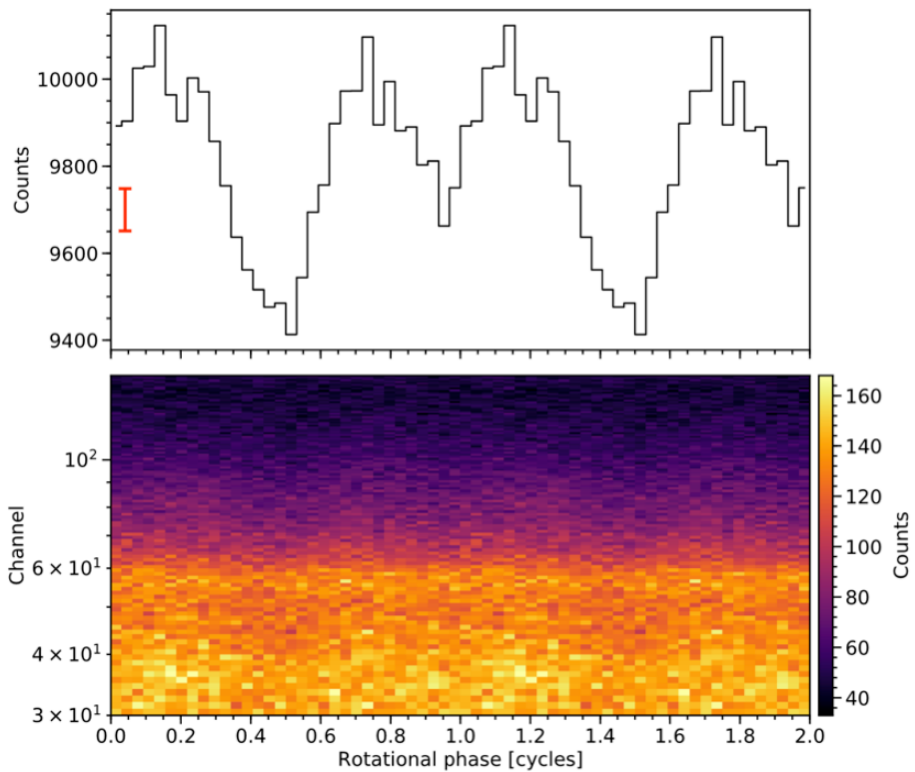
Similar configuration found in Miller et al. 2019,  
but with a third (small) hotspot favored:



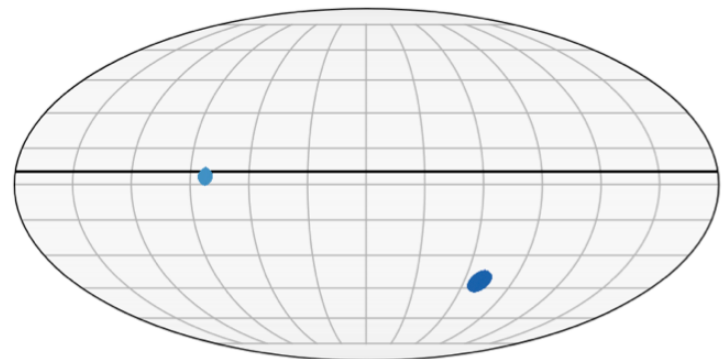
# PSR J0740+6620

A binary millisecond pulsar ( $f = 346$  Hz)  
*Current record holder for most massive PSR*

Riley et al. 2021



Representative hotspot configuration



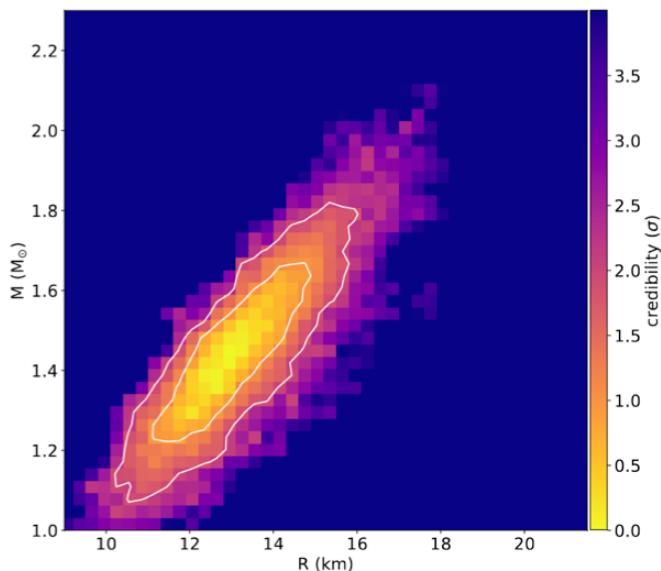
Miller et al. 2021

# J0030+0451

Mass & radius from each group:

■  $M = 1.44^{+0.15}_{-0.14} M_{\odot}$   
 $R_e = 13.02^{+1.24}_{-1.06} \text{ km}$

■  $1.34^{+0.15}_{-0.16} M_{\odot}$   
 $12.71^{+1.14}_{-1.19} \text{ km}$

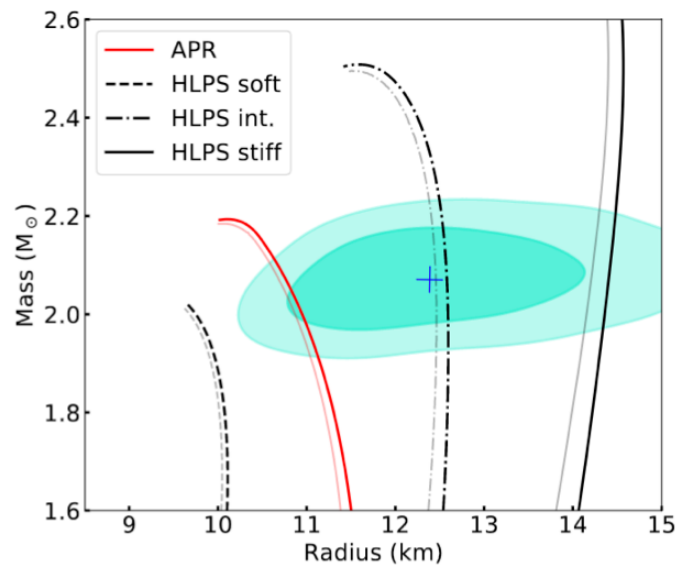


Miller et al. 2019 (figure credit)  
Riley et al. 2019

# J0740+6620

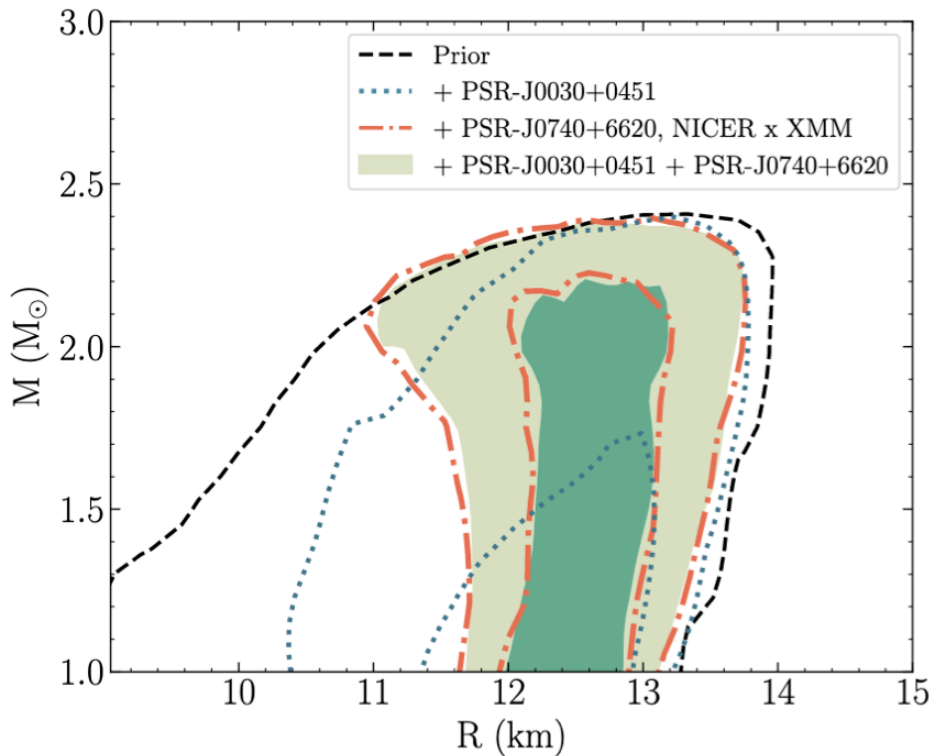
Radius from each group:

■  $13.7^{+2.6}_{-1.5} \text{ km}$  ■  $12.39^{+1.30}_{-0.98} \text{ km}$



Miller et al. 2021  
Riley et al. 2021 (figure credit)

# NICER radii and the NS equation of state



Joint constraints from PSR J0030 and J0740, combined with low-density chiral EFT results from Hebler+ 2013:

$$R_{1.4} = 12.35^{+0.99}_{-1.99} \text{ km}$$

Raaijmakers et al. 2021

# Summary of mass/radius constraints

## Maximum mass constraints

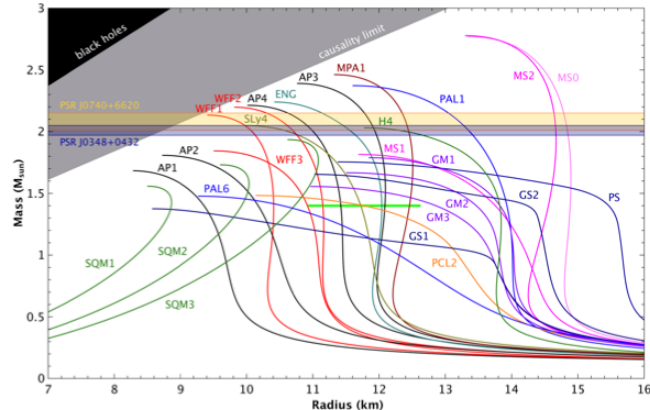
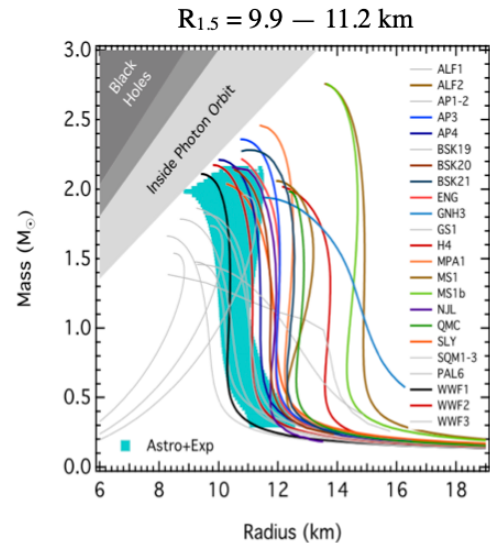


Figure from Dietrich et al. 2020

J0740 constraint: Cromartie et al. 2020,  
Fonseca et al. 2021

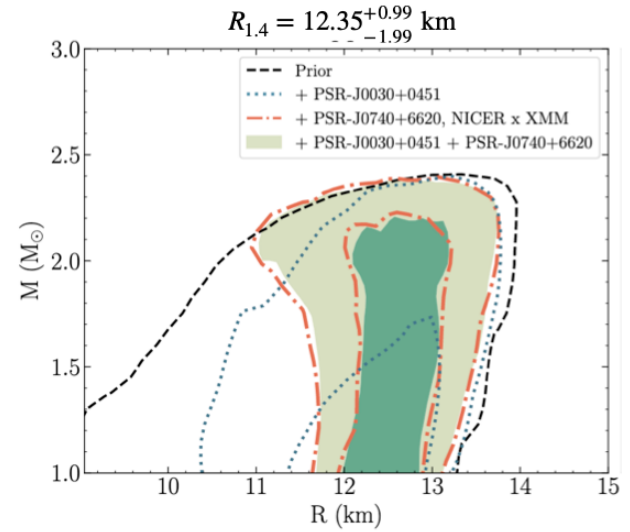
J0348 constraint: Antoniadis et al. 2013

## Spectroscopic radius measurements



Özel & Freire 2016 for a review  
and references therein

## Pulse profile modeling



Raaijmakers et al. 2021;  
Riley et al. 2019, 2021  
Miller et al. 2019, 2021

## **Further reading:**

### **Reviews:**

- Özel & Freire, "Masses, Radii, and Equation of State of Neutron Stars", *Annual Reviews of Astronomy & Astrophysics* (2016)
- Watts et al. "Measuring the neutron star equation of state using X-ray timing", *Reviews of Modern Physics* (2016)
- Lattimer, "Neutron Stars and the Nuclear Matter Equation of State", *Annual Reviews of Nuclear and Particle Science* (2021)